

DOI: 10.47094/COBRAMSEG2024/759

# Geological and geotechnical back analysis of the Punta Cola Rock Avalanche in Chile: A 3-dimensional integrated approach

Ignacio Escudero

Project Geologist, Seequent, Santiago, Chile, ignacio.escudero@seequent.com

Marina Trevizolli

Product Manager, Seequent, Sao Paulo, Brasil, marina.trevizolli@seequent.com

Sergio A. Sepúlveda

PHD Geology, Universidad de Chile, Santiago, Chile, sesepulv@gmail.com

Marisol Lara

MSC Geology, Universidad de Chile, Santiago, Chile, mlara.uchile@gmail.com

**ABSTRACT:** As a result of the earthquake of April 21, 2007, in the Aysén Fjord, Chile, a series of different types of landslides were generated, most of which affected the coastline surrounding the fjord. Among these landslides, a rock avalanche occurred in the Punta Cola sector, which resulted in a rock avalanche that reached the coast and produced a tsunami that affected populated sectors. The main objective of the following work is to perform a back analysis of geological and geotechnical features and compare computation volumes obtained with limit equilibrium analysis and the onshore volume avalanche. All this within an interconnected workflow between implicit modeling for the determination of domains and geometry; and 3D limit equilibrium analysis. The 3D slope stability captured the anisotropic influence on the sliding mass shape, and further comparison with digital elevation post event compared between the computed and observed landslide volumes. This study presents the importance of the proper use of field data on the context of 3D model analysis, the benefits of a combined geological-geotechnical analysis schema and the use of limit equilibrium method for rock failure mechanism driven by discontinuities sets.

**KEYWORDS:** landslides, geological hazard, rock mechanics, 3D slope stability

## 1 INTRODUCTION

The study aims to analyze geological and geotechnical features of the Punta Cola Landslide triggered by the 2007 Aysén's Earthquake, comparing computed volumes using limit equilibrium analysis and onshore volume avalanche. This involves an interconnected workflow combining implicit modeling for domain determination and geometry with 3D limit equilibrium analysis. The study area is located precisely in the vicinity of the Aysén Fjord in the XI region of Chile, south of the capital Santiago, as shown in Figure 1.

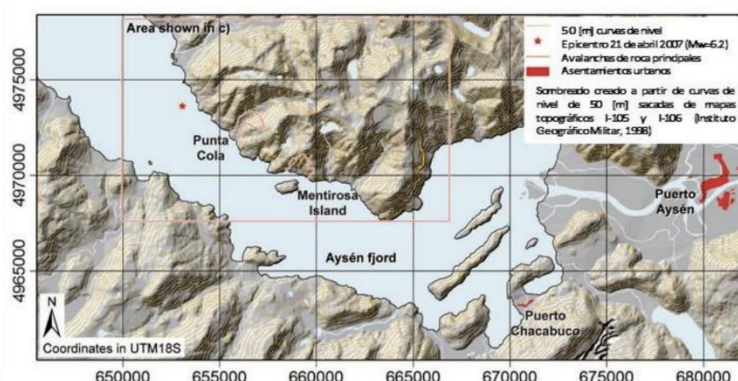


Figure 1. Location of the study area (Escudero, 2017).

## 1.1 Regional and local geology

As previously mentioned, the landslide under study is located at the locality of Punta Cola, to the W of Puerto Aysén. This makes it be subject to the regional geology of the Aysén region, this regional geology is framed within the Southern Andes Volcanic Zone (ZVS), a segment of the Andean orogen located between parallels 33° and 46° S approximately, where there are particular tectonic features, which are manifested, for example, in a volcanism associated with strike-slip type structures (Lara et al., 2008; Cembrano et al., 2002).

The study area is composed of a metamorphic basement (Paleozoic), a sequence of sedimentary units, plutonic rocks and Quaternary deposits. There is a series of sedimentary sequences that interdigitate, showing the processes of the Andean orogen, reaching the base of the stratigraphic column with rocks mainly of marine environment from volcanoclastic to volcano sedimentary. The study area's geology is dominated by the Patagonian Batholith (Mesozoic-Cenozoic), which intrudes the previously described. The Patagonian Batholith is subdivided into three segments according to its spatial position with respect to the north: the North Patagonian Batholith (NPB) located between latitudes 40°-47° S, the South Patagonian Batholith (SPB) defined between latitudes 47°-53° S and finally in the southernmost segment is the Fuegian Batholith (Herve, 2007). In Punta Cola prevails the Norpatagonian Batholith of calc-alkaline plutonic rocks related to a volcanic arc context, intruded in many places by mafic dykes (Beck et al., 2000). The quaternary deposits are classified into 3 groups: morainic deposits, fluvial alluvial deposits, colluvial deposits, and mass removals. Alluvial and fluvial deposits also incorporate glaciofluvial, lacustrine, floodplains, plains, and deltaic materials (Figure 2).

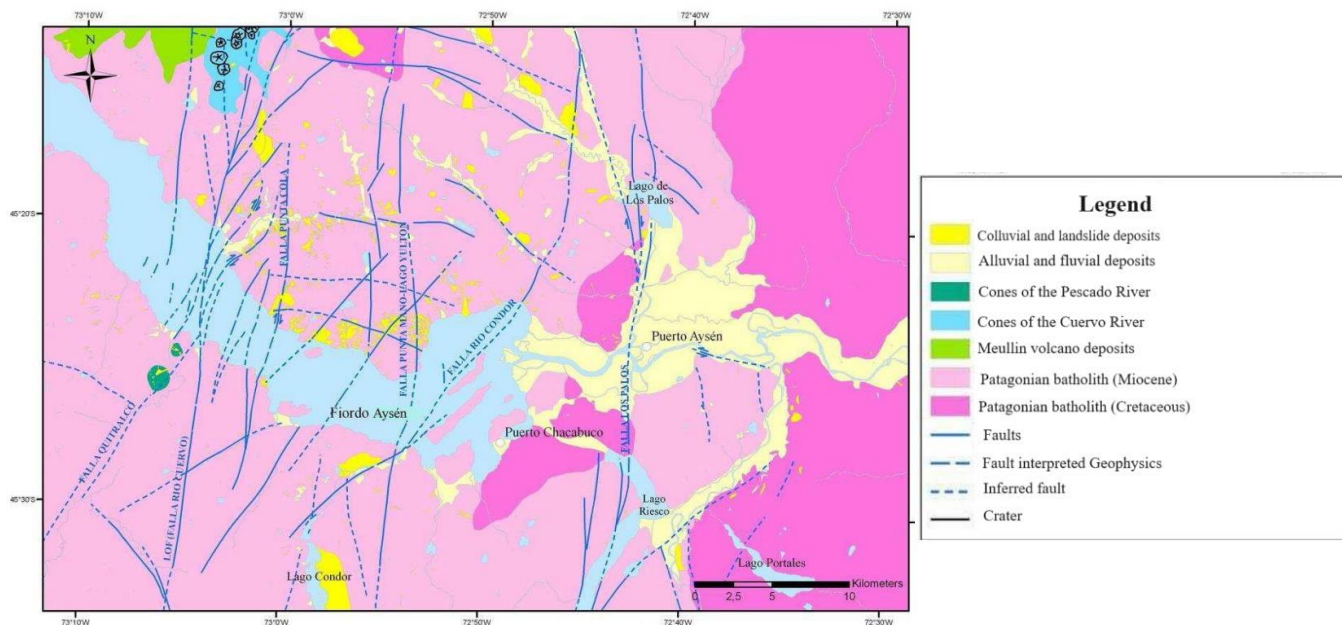


Figure 2. Map of the regional geology of the study area. (Universidad de Chile, 2009).

## 1.2. Aysén Fjord Earthquake 2007

The background of seismicity in the surroundings of the Aysén Fjord is given exclusively by testimonies of locals and information from traditional historiography, which accounts for some events of considerable proportions in the 1920s, including different catastrophic events such as tsunamis (Escudero, 2017).

Notably, the earthquake had a magnitude ( $M_w$ ) of 6.2 (Global CMT Catalog, 2008; NEIC, 2008), whose epicenter was in the vicinity of Punta Cola, west of the town of Puerto Aysén (Figure 3). The hypocenter had a depth of approximately 8 to 9 [km], and a tectonic genesis correlated to one of the LOFZ branches (Vargas et al 2013), in addition to having a high-angle dextral strike slip focal mechanism, according to the National Seismological Center the intensities reported for the towns surrounding Puerto Aysén and Puerto Chacabuco reached a grade of VII on the Mercalli scale (Sepúlveda & Serey, 2009; Naranjo et al., 2009).



### 1.3. Soil and Rock Mass Movements

Mass removals, generated by the seismic event of April 21, 2007, reached 538 events, where the most common were rock-to-soil landslides, with 282 events mapped, followed by 135 landslides, 80 rockfalls, 34 rockslides and avalanches, and 7 debris flows (Serey, 2011). The landslide at Punta Cola was triggered by the 2007 earthquake in Aysén, on a lateral slope of a transverse valley of the NW mantle and continued as an avalanche through the valley until it reached the fjord, with a run-out of about 1 km from the foot of the slope. The flow removed vegetation on the slope opposite the removal, and downstream through the ravine, reaching a run-up height of more than 150 m in the opposite valley (Figure 4).

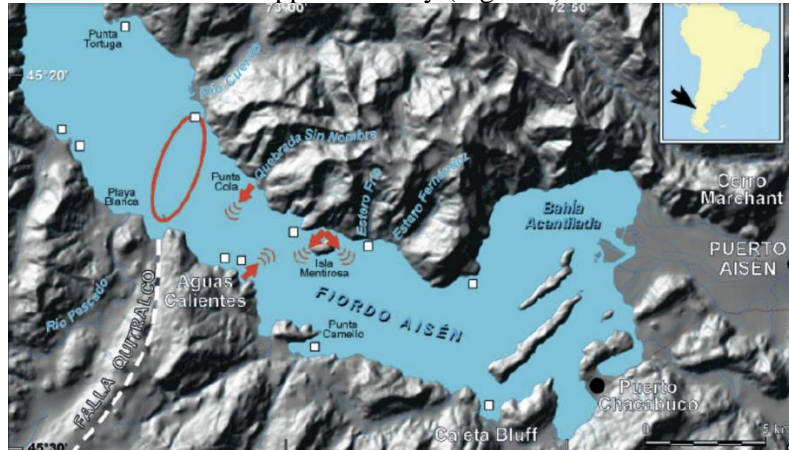


Figure 3. Epicenter of the 2007 Aysén Fjord earthquake (in red ellipse). Red arrows indicate mass removals that reached the fjord (Naranjo et al., 2009).

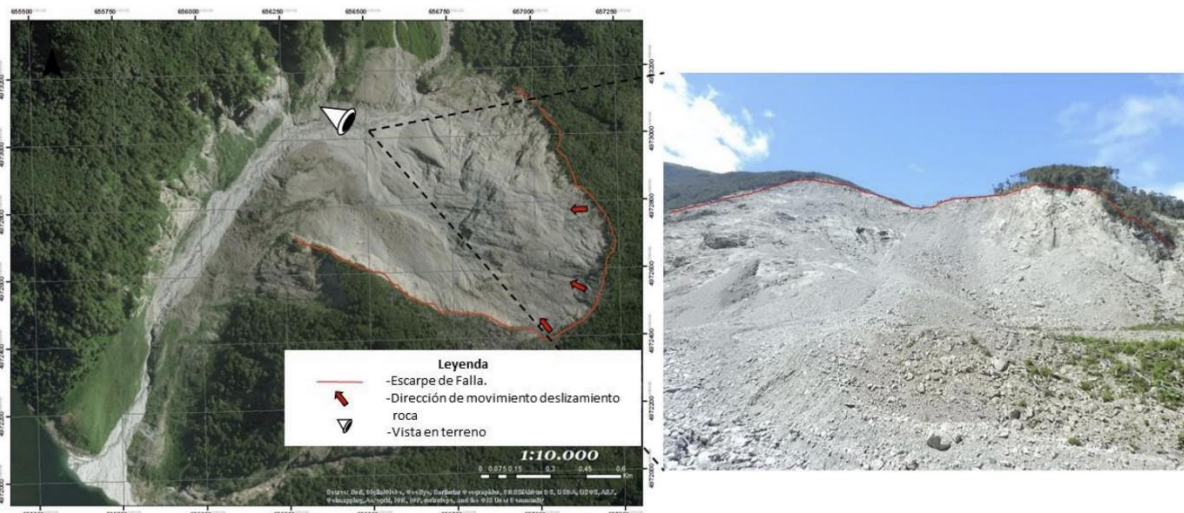


Figure 4. Rockslide of Punta Cola seen in plan (left). SE view of the Punta Cola rockslide (right).

The landslide at Punta Cola occurred on a side slope of a transverse valley of NW mantle, and continued as an avalanche through the valley until it reached the fjord, with a run-out of about 1 km from the foot of the slope. The deposit in the ravine, which extends to the coast of the Fjord, has a variable thickness with a maximum of 20 m, and is located on glacial and alluvial deposits, with this, they reach around 80 m above sea level. This evidence suggests a mechanism of flow of a wave of rock fragments at high velocities, so its classification would be adjusted to that of rockslide or avalanche. In volume, the main slide moved 19.9 Mm<sup>3</sup> of material. In addition, a series of minor removals occurred along the flanks of the valley, which were probably triggered by the friction between the avalanche and the flanks, or perhaps by aftershocks of the main earthquake (Sepúlveda & Serey, 2009; Sepúlveda et al, 2010; Opikkofer et al, 2012).

## 2 METHODOLOGY

The methodology consists of using Leapfrog Works modeling software, from the company Seequent, to be able to visualize all the available information collected from different bibliographic sources and, subsequently, model the geological and geotechnical domains in 3D, in this way the anisotropies that affect the geometry can be observed. Then, using a single source of truth, Central, the 3D model is passed to SLOPE3D for subsequent limit equilibrium stability analysis.

### 2.1. Geotechnical and Geological Domains

For the definition of the geological and geotechnical domains, the information published by Oppikofer *et al.* (2012) was referenced to the digital elevation model and geological and geotechnical observations from field mapping. The integration of such data into a 3D environment eased the geotechnical definition of the 3D anisotropies and lithologies, also, the direct and explicit definition of the discontinuity's sets were fundamental for the subsequent determination of the landslide's morphology (Figure 5).

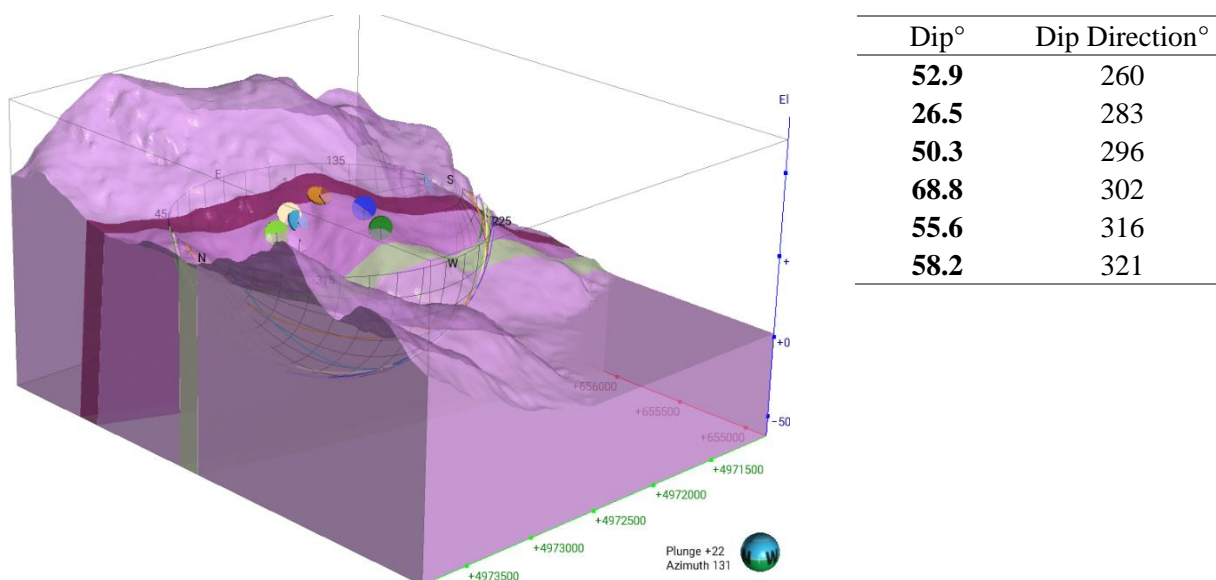


Figure 5. 3D Structure Model and Geomorphology with Dip and Dip direction of join sets.

The sets of discontinuities are distributed in two zones: BFS (Basal Failure Surface) and LRS (Lateral Release Surface), as is shown in Figure 5.

Based on data collected by Escudero (2017) and combined with structural information and anisotropies, the geotechnical domains for back analysis using limit equilibrium were defined. These domains (Figure 5) identify the batholith as the primary rock mass unit, based on lithology. Additionally, geomorphology complements by defining a distinct resistance zone known as the Highly Fractured Zone (HFZ), previously mapped by Oppikofer *et al.* (2012). Structural mapping also reveals a fault zone at the slope's base, called the Punta Cola Fault Zone (PCFZ).

Additionally, the geotechnical properties are defined, as extracted from Escudero (2017). In the case of material models, the Howk-Brown constitutive model is used according to the following parameters in Table 1. The joint sets, representing the structures through the Mohr Coulomb model, shown in Table 2.

The material models used in the analysis for all the materials was Compound Strength (GeoStudio, 2024). This is a type of model where is necessary define 2 distinct models to use: a Base Material and Joint

Parameters. The model is going to make a composite with the slip surface and choose in between these two materials according to the geometrical and tolerance information given.

For the seismic input, the PGA in both horizontal and vertical component, were chosen from the conservative case shown in Escudero (2017) whose values are display in Table 2. For the designation of the Seismic Coefficient (k) 0.5 of the value of the PGA was used in both components.

Table 1. Hoek-Brown model information used in the constituent models of 3D limit equilibrium analysis (Escudero, 2017).

Unit	GSI	a	mi	mb	s	UCS kPa	$\sigma_3$ kPa
Batolito	50	0.5	33	5.533	0.003865	150,000	100,000
PCFZ	35	0.5	33	3.2384	0.0007	100,000	210000
HFZ	35	0.5	33	3.2384	0.0007	100,000	210000

Table 2. Mohr Coulomb model information for 3D limit equilibrium analysis discontinuities and seismic input (Escudero, 2017).

Parameter	Value
Friccion Angle	33°
Cohesion	10 kPa
Unit Weight	28 kN/m <sup>3</sup>
PGA H	1.2
PGA V	0.6

### 3 RESULTS AND DISCUSSIONS

The slope stability results are displayed in Figure 6, performed in the SLOPE3D software. Two base cases were performed, one Static and the other Pseudo-static. Both critical surfaces were optimized with the algorithm of the software and analyzed with Morgenstern-Price. Static case used Cuckoo search for a broader evaluation of the area and Entry and Exit covering the critical sliding mass observed after the earthquake event.

The results highlight the complex structures and mechanisms involved earthquake-triggered landslides and driving forces on the minimum factor of safety. The 3D slope stability captured the anisotropic influence on the sliding mass shape, and further comparison with digital elevation post event compared between the computed and observed landslide volumes.

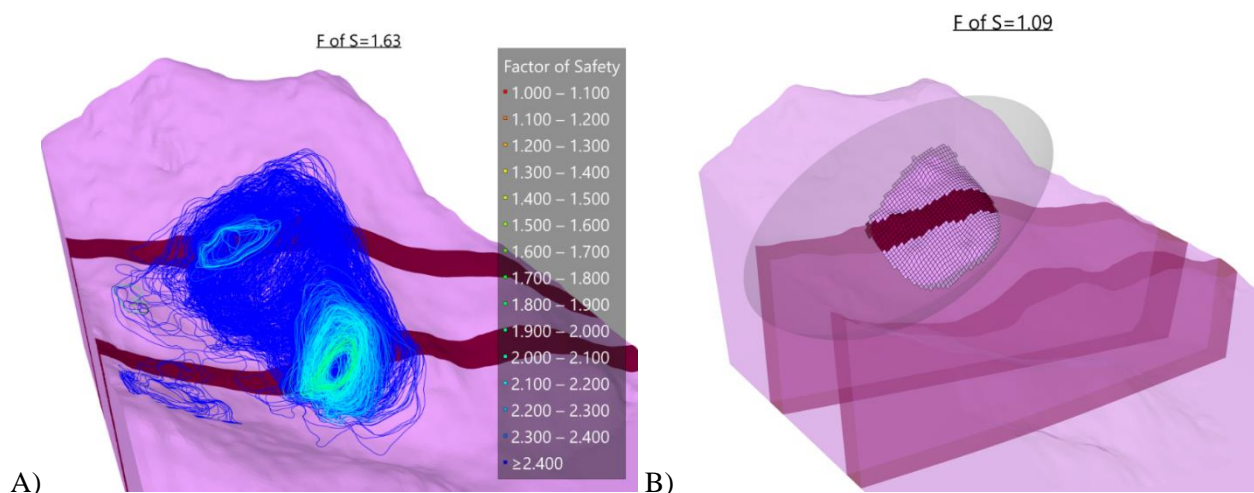


Figure 6. Analysis Results 3D Limit Equilibrium A) Static Case B) Pseudo-Static Case



**Table 3. Summary of slope stability analysis definition and results**

Parameter	Static Case	Pseudo-Static Case
Factor of Safety	1.63	1.09
Kv/Kh	no	0.5
Volume	13,942 m <sup>3</sup>	31.213 Mm <sup>3</sup>

The dynamic nature of the earthquake poses a challenge for the analysis of seismicity-triggered mass removals. Since the responses of the inertial forces along with the generated displacement, therefore, it is a representation that may be necessary to complete the analysis. The Static case shows a factor of safety greater than 1 indicating stability, as well as delivering the zones where the fault surfaces are distributed, which are in the study area and coincide with the fault scarp. On the other hand the Pseudo Static case shows that is at a critical safety factor, of almost 1 which means at failure (Figure 6). A comparison that might be indicated at first glance is the fact that the factor of safety is lower for the Pseudo Static case, which alongside the fact that the factor of safety is almost 1, is consistent with incorporating seismic forces into the direction of motion and would also characterize the fault as earthquake-triggered.

The breakup sequence of the rock avalanche could be further evaluated since the limit equilibrium method, by its nature, provides a single surface where computation and iteration take place. In other words, and for the Pseudo Static scenario, the sliding surface is a single one, without giving rise to a set of surfaces that could be triggered non-simultaneously, which was the case of the removal of Punta Cola, or also give rise to a surface that could be smaller than the observed escarpment, but that converges because it follows the criterion of safety factor. This could result in a representation that encompasses all the other threads that exist at the time of removal on a volume, or the volume could result in a smaller surface area, the product of an additional thread to the main one. Precisely the 3D analysis allows segmenting in a representative way the different fault zones. The incorporation of anisotropy surfaces extracted from the joint sets and worked for their transformation into planes that deliver the anisotropy in Leapfrog allowed to deliver a direct component that is to carry the trend of the discontinuities and give a representative fault surface in volume and direction, as well as the failure mechanisms to ensure rupture. All this without going through a projection to the 2D geometry where the intersection and final behavior is lost. This is why explicitly importing the representative planes of the anisotropies could improve the definition of the surface for a case of back analysis like the current one. Another topic that is not being represented in the method of limit equilibrium is the propagation of the wave of the earthquake, which can lead to site and amplification, generating an amplification of the signal.

For the static case, the volume comparison could be misleading, since it would be comparing a case that was not previously available and with no representativeness. In contrast, in the pseudo-static case it can be observed that it is within the order of magnitude of the volume calculated for the rock avalanche of 22.4 Mm<sup>3</sup>, but as shown in the Table 3, the volume obtained by the limit equilibrium in 3D is greater, being an approach that takes a larger surface and makes the entire slope of the gully subject to the fault, which gives it a more conservative character, as a first approach the limit equilibrium analysis already has a failure mechanism and a sequence that yields with more conservative analyses, and also an approximated volume of failure.

### 3 CONCLUSION

This study presents the importance of the proper use of field data in the context of three-dimensional model analysis, the advantages of a combined geological-geotechnical analysis scheme, and the use of the limit equilibrium method for rock failure mechanisms caused by sets of discontinuities. The limit equilibrium method provides regions and zones where the failure could happened an approximated volume of failure, all this information is fundamental and works as a conservative first approach. The limitations of the limit equilibrium are given by not considering the chronology of rupture or all the steps that would take for the slide to failed; another topic not considered is the effect of site and amplification, which can amplified the signal in the geometry of analysis. The 3-dimensional analysis provides a focus where the structures can explicitly be visualized and used for computing, which generates a final surface more representative for the back analysis.

## ACKNOWLEDGMENT

Thanks to the FONDECYT Project 1140317 "Dynamic response and stability of large rock slopes during earthquakes" and to the Seequent team in Latin America and the world for their support during the realization of this article.

## REFERENCES

- Beck, M.E., Burmester, R., Cembrano, J., Drake, R., Garcia, A., Hervé, F., Munizaga, F., 2000. Paleomagnetism of the North Patagonian batholith, southern Chile. An exercise in shape analysis. *Tectonophysics*, 326, 185–202.
- Cembrano, J. Lavenu, A., Reynolds, P., Arancibia, G., López, G., Sanhueza, A., 2002. Late Cenozoic ductile deformation north of the Nazca-South America-Antarctica triple junction. *Tectonophysics*, 354, 289-314.
- Charrier, R; Pinto, L.; Rodríguez, M.P. 2007. Tectonostratigraphic evolution of the Andean Orogen in Chile. In *The Geology of Chile* (Moreno, T; Gibbons, W.; editors). The Geological Society of London: 21-114. London.
- De la Cruz, R, Suárez, M., Belmar, M., Quiroz, D. Y Bell, M. 2003. Área Coyhaique – Balmaceda, Región de Aisén de General Carlos Ibáñez de Campo. Servicio Nacional de Geología y Minería, Carta Geológica de Chile, Serie Geológica Básica, No. 80, 40 p., 1 mapa escala 1:100.000.
- De la Cruz, R. y Suarez, M. 2006. Geología del Área Puerto Guadal – Puerto Sánchez, Región de Aisén de General Carlos Ibáñez de Campo. Servicio Nacional de Geología y Minería, Carta Geológica de Chile, Serie Geológica Básica, No. 95, 85 p., 1 mapa escala 1:100.000.
- Escudero, I., 2017. Modelamiento dinámico mediante elementos discretos del deslizamiento de roca de Punta Cola generado por el terremoto del Fjordo Aysén del 2007. Tesis para optar al grado de magister en ciencias mención geología. Departamento de geología. Universidad de Chile.
- GeoStudio, 2024. GeoStudio Slope Stability Modeling Manual. [https://lms.seequentlearning.com/learner\\_resource\\_list](https://lms.seequentlearning.com/learner_resource_list)
- Naranjo, J.A., Arenas, M., Clavero, J., Muñoz, O. 2009. Mass movement-induced tsunamis: main effects during the Patagonian Fjordland seismic crisis in Aisén (45°25'S), Chile. *Andean Geology*, 36, 137-146.
- Niemeyer, H., Skarmeta, J., Fuenzalida, R. and Espinoza, W. 1984. Hoja Península de Taitao y Puerto Aysén. Carta geológica de Chile N° 60-61, SERNAGEOMIN, Santiago, Chile, 80 pp. 132
- Oppikofer, T., Hermanns, R., Redfield, T., Sepúlveda, S., Duhart, P., Bascuñan, I. 2012. Morphologic description of the Punta Cola rock avalanche and associated minor rockslides caused by the 21 april 2007 Aysén earthquake (Patagonia, southern Chile). *Revista de la Asociación geológica Argentina* 69 (3): 339 - 353 (2012)
- Sepúlveda, S.A. and Serey, A. 2009. Tsunamigenic, earthquake-triggered rock slope failures during the April 21, 2007 Aisén earthquake, southern Chile (45.5°S). *Andean Geology* 36: 131-136. doi:10.4067/S0718-71062009000100010.
- Sepúlveda, S.A., Serey, A., Lara, M., Pavez, A. and Rebolledo, S. 2010. Landslides induced by the April 2007 Aysén fjord earthquake, Chilean Patagonia. *Landslides* 7: 483-492. doi:10.1007/s10346-010-0203-2

Serey, A. 2011. Análisis de las remociones en masa generadas por el terremoto del Fiordo Aysén de 2007 (45,5°S). Tesis para optar al grado de magister en ciencias mención geología. Memoria para optar al título de geología. Departamento de geología. Universidad de Chile.

SERNAGEOMIN, 2003. Mapa Geológico de Chile: versión digital. Servicio Nacional de Geología y Minería, Publicación Geológica Digital, No. 4. Santiago.

Universidad de Chile. 2009. Línea de base Estudio de Impacto Ambiental "Proyecto Central Hidroeléctrica Cuervo". <http://seia.sea.gob.cl/documentos/documento.php?idDocumento=3965520>

Vargas, G., Rebolledo, S., Sepúlveda, S., Lahsen, A., Thiele, R., Townley, B., Padilla, C., Rauld, R., Herrera, M., Lara, M. 2013. Submarine earthquake rupture, active faulting and volcanism along the major Liquiñe-Ofqui Fault Zone and implications for seismic hazard assessment in the Patagonian Andes. *Andean Geology* 40 (1): 141-171. January, 2013 doi: 10.5027/andgeoV40n1-a07